Available online at www.sciencedirect.com

SciVerse ScienceDirect

Ceramics International 39 (2013) 6835–6840

CERAMICS INTERNATIONAL

www.elsevier.com/locate/ceramint

Luminescence properties of Eu^{2+} and Ce^{3+} ions in calcium lithio-germanate Li_2CaGeO_4

I.V. Berezovskaya[a], N.P. Efryushina[a], I.I. Seifullina[b], E.E. Martsinko[b], B.I. Zadneprovski[c], G.B. Stryganyuk[d,e], A.S. Voloshinovskii[d], S.M. Levshov[a], V.P. Dotsenko[a,*]

[a]*A.V. Bogatsky Physico-Chemical Institute, National Academy of Sciences of Ukraine, Lustdorfskaya doroga 86, 65080 Odessa, Ukraine*
[b]*Mechnikov Odessa National University, Dvoryanskaya 2, 65082 Odessa, Ukraine*
[c]*Central Research and Development Institute of Chemistry and Mechanics, 115487 Moscow, Russia*
[d]*Ivan Franko National University of Lviv, Kirilo i Mefodii 8, 79005 Lviv, Ukraine*
[e]*HASYLAB at DESY, Notkestraße 85, 22607 Hamburg, Germany*

Received 16 January 2013; accepted 8 February 2013
Available online 14 February 2013

Abstract

The Eu^{2+}-doped Li_2CaGeO_4 samples have been prepared by the solid state reaction method and by thermolysis of the complex precursor. It was shown that Eu^{2+} ions in Li_2CaGeO_4 exhibit an intense emission with a maximum at 473 nm. The Stokes shift (820 cm^{-1}) and full-width at half-maximum (1415 cm^{-1}) of the emission band are close to those of the Eu^{2+} emission in Li_2CaSiO_4. Values of the crystal field splitting and the centroid shift of the Ce^{3+} 5d configuration in Li_2CaGeO_4 were also determined and compared with those of Ce^{3+} ions in Li_2CaSiO_4. Although the spectral positions of the Ce^{3+} lowest excitation band for Li_2CaRO_4 (R=Si, Ge) are practically the same, the magnitudes of the Ce^{3+} crystal field splitting appeared to be unexpectedly very different. This effect is tentatively attributed to a strong distortion of the calcium site in Li_2CaSiO_4 caused by the presence of the trivalent lanthanide ion.

Keywords: A. Powders: chemical preparation; B. Spectroscopy; C. Optical properties; E. Functional applications

1. Introduction

In recent years, several alkaline earth silicates doped with lanthanides (Ln), such as $Sr_3SiO_5:Ce^{3+},Li^+$ [1], $Ca_3Si_2O_7:Eu^{2+}$ [2], $M_2MgSi_2O_7:Eu^{2+}$ (M=Ca, Sr, Ba) [2,3], and $Li_2MSiO_4:Eu^{2+}$ (M=Ca, Sr, Ba) [4–7], have been presented as promising phosphors for white light-emitting diodes (LEDs) and field emission displays (FEDs). Among these series, materials of composition $Li_2MSiO_4:Eu^{2+}$ (M=Ca, Sr) gained special attention because of their favorable luminescence properties and a weak thermal quenching of luminescence. Several groups of authors have studied the luminescence properties of Eu^{2+} ions in Li_2MSiO_4 (M=Ca, Sr) upon optical and synchrotron excitations [2,4–9]. It was found that Eu^{2+}-doped Li_2MSiO_4 (M=Ca, Sr) shows broadband emissions with a maximum at about 478 and 575 nm. Since the emission of $Li_2SrSiO_4:Eu^{2+}$ is efficiently excited by photons in the 380–420 nm region, quite efficient white LEDs were fabricated by using a combination of this material as a yellow–orange phosphor and (In,Ga)N chips emitting around 420 nm [4,5]. In comparison with silicates, luminescence properties of Eu^{2+} and Ce^{3+} ions in alkaline earth germanates gained less attention, probably, due to their low luminescence efficiency in some germanates. This observation was attributed to photoionization of impurity ions caused by a relatively small band gap of germanate hosts [10]. However, Jiang et al. [11] have recently reported that Ce^{3+} ions in Ca_2GeO_4 exhibit a very efficient yellow emission with a maximum at about 560 nm upon excitation by a radiation from (In, Ga)N-based blue LEDs. These authors came to the conclusion that $Ca_2GeO_4:Ce^{3+}$, Li^+ is a promising phosphor for LEDs applications. Also, Jian-Xin et al. [12] have studied

*Corresponding author. Tel.: +380 487659227; fax: +380 487659602.
E-mail address: ssclab@ukr.net (V.P. Dotsenko).

0272-8842/$ - see front matter © 2013 Elsevier Ltd and Techna Group S.r.l. All rights reserved.
http://dx.doi.org/10.1016/j.ceramint.2013.02.015

luminescence properties of Ce^{3+} and Dy^{3+} ions in Li_2CaGeO_4 upon excitation in the range 270–450 nm and revealed the presence of efficient energy transfer between Ce^{3+} and Dy^{3+} ions in this host lattice.

To the best of our knowledge, the luminescence properties of Eu^{2+} ions in Li_2CaGeO_4 have not been reported up to now. In this work, we have compared the luminescence characteristics of Eu^{2+} ions in Li_2CaGeO_4 and its structural analog—Li_2CaSiO_4. Also, the measurements on Ce^{3+}-doped Li_2CaGeO_4 have been extended into the vacuum-ultraviolet (VUV) spectral region. It is known that Li_2CaGeO_4 is isostructural with Li_2CaSiO_4 and their crystal structures comprise columns, parallel to (001) plane, of alternating calcium polyhedra and GeO_4 (or SiO_4) tetrahedra that are linked by sharing edges [13]. The lithium atoms are in distorted (LiO_4) tetrahedra joined at the corners to form sheets perpendicular to (001) plane. In these compounds each Ca atom is coordinated by eight oxygen atoms forming a dodecahedron (D_{2d} point symmetry) with four long Ca–O distances of 2.737 (2.686 Å) and four short Ca–O distances of 2.388 Å (2.408 Å) for Li_2CaGeO_4 and its Si-analog, respectively [13].

2. Experimental

Polycrystalline samples of general composition $Li_2Ca_{1-x}Ln_xGeO_4$ (Ln = Eu^{2+}, Ce^{3+}; x = 0.001–0.01) were prepared by a solid state reaction method. Starting mixtures of $CaCO_3$ (99.9%), Li_2CO_3 (2.5% excess, 99.5%), GeO_2 (99.9%), SiO_2 and Eu_2O_3 or CeO_2 (99.99%) were fired at a temperature of about 700 °C for 1 h in air and 930 °C for 3 h in a reducing medium created by burning activated carbon. The specimens were cooled, mortared to insure homogeneity and fired again at 930 °C for 3–5 h in a reducing medium of CO. The synthesis procedure of Eu-doped Li_2CaSiO_4 was described earlier in Ref. [9].

Taking into account the well-known shortcomings of the solid state reaction method, such as a large grain size of final products, differences in activator (e.g. Ln) concentrations within the grains and in the vicinity of grain boundaries, the sample of composition $Li_2Ca_{1-x}Eu_xGeO_4$ (x = 0.01) was also prepared using a complex precursor consisting of calculated quantities of cation–anion complex $[Ca(H_2O)_6][Ge(HCitr)_2]$ and lithium carbonate. The complex was synthesized by the building blocks method with the use of biscitrate germanium acid and calcium carbonate as reagents. The synthesis procedure was analogous to that described earlier in Ref. [14]. The precursor was then subjected to two-stage heat treatment at 700 °C for 1 h and 900 °C for 3 h. The temperature regions of the precursor decomposition and formation of Li_2CaGeO_4 were evaluated using the data of differential thermal analysis (DTA) which was performed on a thermal analyzer (LABSYS DSC/DTA/TG) in air at a heating rate of 10 °C/min. The samples were checked by X-ray diffraction (XRD) using Cu K_α radiation (Rigaku Ultima IV). The particle size distribution was obtained by the laser diffraction method using a Shimadzu SALD 2201 analyzer. The emission and excitation spectra in the UV–visible region were recorded at 77 K and room temperature on a Fluorolog Fl-3 (Horiba Jobin Yvon) spectrofluorometer equipped with a xenon lamp. The excitation spectra at wavelengths shorter than 330 nm and the luminescence decay kinetics were recorded at room temperature using synchrotron radiation and the equipment of the SUPERLUMI experimental station [15] of HASYLAB (Hamburg, Germany). The excitation spectra were corrected for the wavelength dependent excitation intensity with the use of sodium salicylate as a standard.

3. Results

As mentioned above, in order to study the behavior of the precursor upon heating, differential-thermal analysis was used. TG and DTA curves of the precursor are presented in Fig. 1. As can be seen, the DTA curve shows several endothermic and exothermic effects, with a total mass loss of about 69%. This value is close to the theoretical mass loss (71%) of the precursor. The endothermic peaks at 100 and ~250 °C correspond to release of adsorbed and chemically bonded water, respectively. The second mass loss (34.6%) lying from 250 to 400 °C is also associated with endothermic effects. This stage can be assigned to the thermolysis of the organic part of the precursor. The third stage of mass loss is associated with several exothermic effects, the most intense of which is at 524 °C. Above 750 °C only a small mass loss takes place. Most probably, this is related to the removal of the residual carbon-containing groups embedded in Li_2CaGeO_4. Furthermore, there is a relatively strong exothermic effect at about 800 °C, which reflects the onset of Li_2CaGeO_4 formation.

The XRD patterns of the final products prepared by solid state reactions appeared to be well matched with JCPDS File no. 27-0289 for Li_2CaGeO_4. No impurity phases were detected in the XRD patterns of these samples, whereas the pattern of the sample prepared using the precursor revealed, in addition to Li_2CaGeO_4, the presence of a small amount

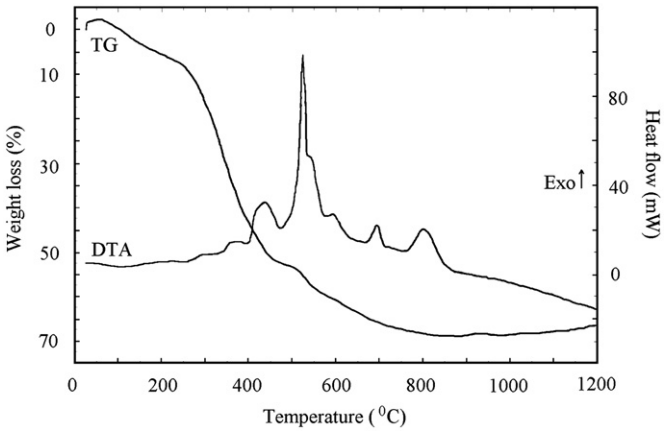

Fig. 1. TG and DTA curves of the precursor used for the preparation of Li_2CaGeO_4.

of unknown phase (see Fig. 2). The particle size distribution of Li_2CaGeO_4 prepared with the use of the precursor is shown in Fig. 3. It is seen that the size of majority of the particles does not exceed 1 μm. The average size of crystallites (*d*) was found to be 480 nm. This value is essentially smaller than typical ones (2–20 μm) for alkaline earth silicates and germanates prepared by solid state reactions [5,10]. The narrow particle size distribution and relatively small value of *d* are generally favorable for possible applications of the as-prepared material as a phosphor.

The emission and excitation spectra for Eu-doped Li_2CaGeO_4 ($x=0.01$) samples prepared by the two different methods appeared to be identical. Moreover, no significant difference in emission intensity was observed between these samples. As can be seen from Fig. 4, upon excitation at 370 nm the emission spectrum of $Li_2Ca_{1-x}Eu_xGeO_4$ ($x=0.01$) consists of an intense band peaking at about 473 nm with a full-width at half-maximum of 1415 cm^{-1}. One can expect that this band is due to $4f^65d \rightarrow 4f^7$ transition of Eu^{2+}, because Eu^{2+} ions in Li_2CaSiO_4 show a similar emission with a maximum at 478 nm [6,8]. Upon excitation at 240 nm the emission spectrum contains also several groups of bands in the range 578–710 nm. No doubt that these features are due

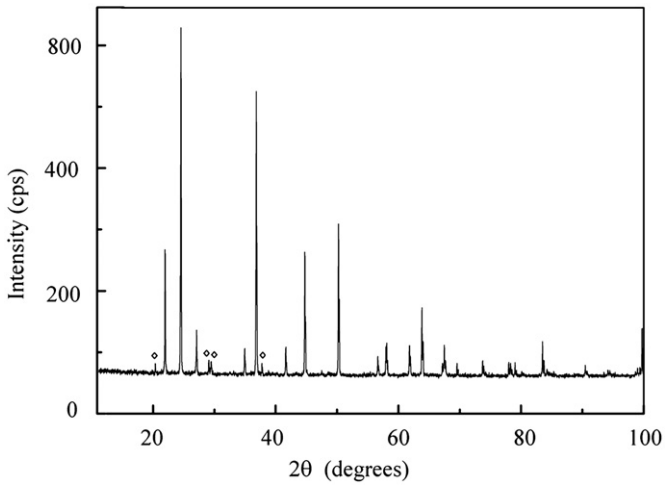

Fig. 2. Powder X-ray diffraction pattern of Li_2CaGeO_4 prepared with the use of the precursor. Nonidentified peaks are denoted by the symbols (◇).

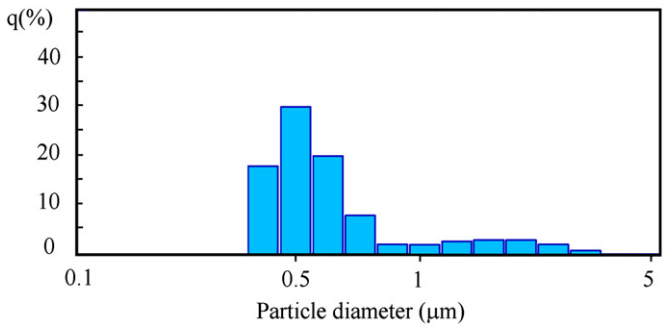

Fig. 3. Particle size distribution of Li_2CaGeO_4 prepared with the use of the precursor.

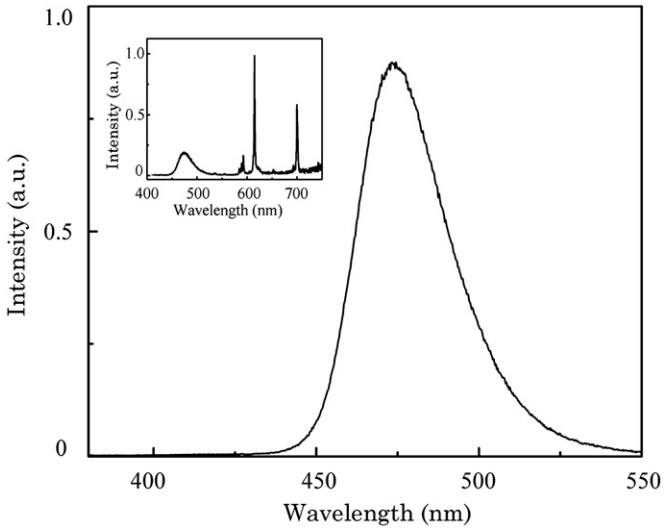

Fig. 4. Emission spectrum of $Li_2Ca_{1-x}Eu_xGeO_4$ ($x=0.01$) recorded upon excitation at 370 nm. The inset shows the emission spectrum upon excitation at 240 nm.

to the $^5D_0 \rightarrow {}^7F_j$ ($j=0$–4) transitions of Eu^{3+} ions. Thus, the stabilization of Eu^{2+} in Li_2CaGeO_4 during the synthesis process requires a strong reducing agent, even then depending upon the preparation conditions some amount of Eu^{3+} can be revealed in the final products. The same conclusion was made previously for Eu^{2+} ions in Li_2MSiO_4 (M = Ca, Sr) [6,7]. Note that since both the formal charge and ionic radius of Eu^{2+} and Eu^{3+} ions differ markedly from those of Li^+, it seems rather unprobable that $Eu^{2+/3+}$ ions can substitute for Li^+ in any significant amounts.

Fig. 5 shows the excitation spectra for the Eu^{3+} emission recorded upon excitation with synchrotron radiation and optical photons. They consist of a broad band with a maximum at about 241 nm and a number of relatively narrow bands at the longer wavelengths. It is clear that the intense band is caused by the charge transfer (CT) transition from the oxygen 2p states to the empty states of the Eu^{3+} $4f^6$-configuration, while the weaker ones are due to the $4f^6 \rightarrow 4f^6$ transitions of Eu^{3+} ions. Note that the observed position of the Eu^{3+} CT band in Li_2CaGeO_4 ($\lambda_{max}=241$ nm) is close to those of Eu^{3+} in Li_2MSiO_4 (M = Ca, Sr) ($\lambda_{max}=238$ and 243 nm [7]), which also contain in their structures eight coordinated Ca (Sr)-atoms. In the vacuum UV (VUV) excitation spectrum (curve a), there are also some features in the 100–170 nm region. Their possible origin will be discussed below.

The excitation spectra of $Li_2Ca_{1-x}Eu_xRO_4$ (R = Si, Ge; $x=0.01$) at 77 K for the Eu^{2+} emissions at 470 nm are compared in Fig. 6. Both the spectra consist of several overlapping bands in the range 250–475 nm, which are due to excitation of the Eu^{2+} ions via transitions from the $4f^7$ ($^8S_{7/2}$) ground state to the components of the Eu^{2+} $4f^65d$ configuration. The low energy tails of these spectra exhibit fine structure, which probably reflects the character of the seven (Eu^{3+}) $4f^6$ levels ($^7F_{0-6}$). The spectra, presented in

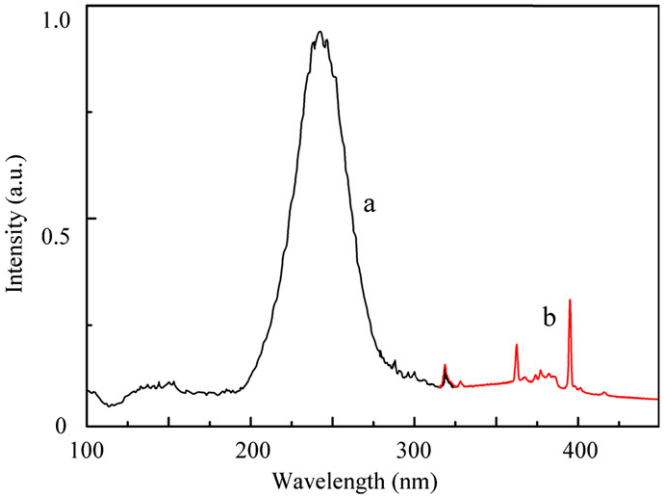

Fig. 5. Excitation spectra of $Li_2Ca_{1-x}Eu_xSiO_4$ ($x=0.01$) for the Eu^{3+} emission ($\lambda_{em}=612$ nm) at 293 K. The spectra were recorded upon excitation with synchrotron radiation (curve a) and optical photons (curve b).

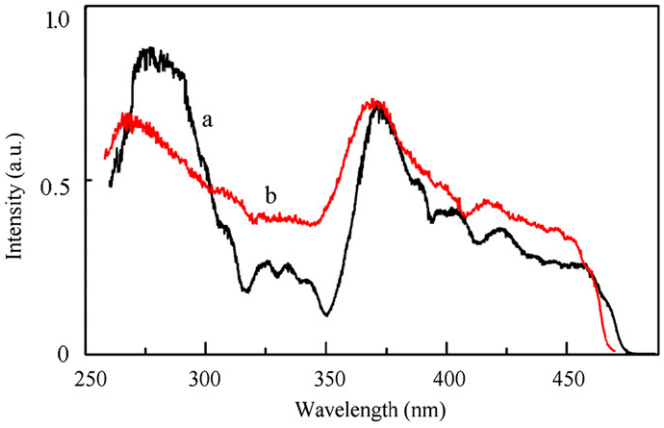

Fig. 6. Excitation spectra of $Li_2Ca_{1-x}Eu_xRO_4$ (R=Ge (a), Si (b); $x=0.01$) for the Eu^{2+} emissions at 470 nm at 77 K.

Fig. 6, are quite similar with the exception of slight shift (by 2–6 nm) of the $Li_2Ca_{1-x}Eu_xGeO_4$ excitation maxima toward shorter wavelengths. It is difficult to determine exactly the Stokes shift (δ) of the Eu^{2+} emission in Li_2CaGeO_4, because the lowest-energy excitation band can be too weak to be observed. In view of this, the value of δ was roughly determined from the energy of the zero phonon line, which can be taken as the intersection point of the normalized excitation and emission bands. For Eu^{2+}-doped Li_2CaGeO_4, the overlap of the excitation and emission spectra occurs at about 463 nm. In this way the Stokes shift of the emission ($\lambda_{max}=472$ nm at 77 K) was found to be 820 cm^{-1}. This value is very close to that ($\delta=850$ cm^{-1}) reported previously for the Eu^{2+} emission in Li_2CaSiO_4 [9].

Fig. 7 shows the emission and excitation spectra of $Li_2Ca_{1-x}Ce_xGeO_4$ ($x=0.001$). The emission band extends from 350 to 425 nm and has two maxima at about 366 and

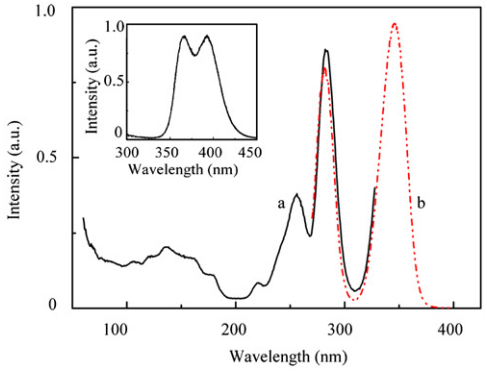

Fig. 7. Excitation spectra of $Li_2Ca_{1-x}Ce_xGeO_4$ ($x=0.001$) for the Ce^{3+} emission at 370 nm at 293 K. The spectrum is a superposition of curves (a) and (b) obtained upon excitation with synchrotron radiation and optical photons, respectively. The inset shows the emission spectrum upon excitation at 345 nm.

393 nm. Their position is practically independent on the excitation wavelength. It is evident that these maxima are due to transitions from the lowest Ce^{3+} 5d excited state to the 4f ground state levels $^2F_{5/2}$ and $^2F_{7/2}$. The excitation spectra for this emission at 293 K (curves a and b) consist of bands at 219, 237, 256, 282 and 346 nm, which are due to direct excitation of the Ce^{3+} ions via transitions to the components of the Ce^{3+} 5d configuration. The lowest excitation band is situated at 346 nm, so that the Stokes shift (δ) of the Ce^{3+} emission in Li_2CaGeO_4 amounts to 1580 cm^{-1}. Since no significant change of the Ce^{3+} emission in $Li_2Ca_{1-x}Ce_xGeO_4$ is observed upon varying the Ce^{3+} concentration in the range $x=0.001$–0.005, one can conclude that most of the Ce^{3+} ions are present in the form of locally uncompensated Ce^{+}_{Ca} centers. However, for higher x, the formation of Ce^{3+} centers, locally compensated by point defects, can be expected. In the above-mentioned study by Jian-Xin et al. [12], the maxima of the Ce^{3+} emission in $Li_2Ca_{1-x}Ce_xGeO_4$ ($x=0.01$) have been recorded at 372 and 400 nm. This somewhat differs from that found in the present work. This discrepancy can be explained by the existence of several kinds of cerium centers in the sample with the higher Ce^{3+} concentration studied by Jian-Xin et al. [12].

As seen from Fig. 7, in addition to the 4f→5d excitation bands, the excitation spectrum contains several overlapping bands in the 100–180 nm range with local maxima at about 180, 163 and 136 nm, which were also observed in the excitation spectra for the emission of $Eu^{3+/2+}$-doped Li_2CaGeO_4. These features can be attributed to host lattice absorption with a subsequent energy transfer to the Ce^{3+} ions. This interpretation is supported by the results of decay time-measurements on $Li_2Ca_{1-x}Ce_xGeO_4$ ($x=0.001$). Upon excitation at $\lambda_{exc}=288$ nm the decay was found to be exponential with a time constant of 30 ± 1 ns. This value is typical for Ce^{3+} 5d→4f transitions. Upon excitation at $\lambda_{exc}=160$ nm the decay showed a distinct deviation from the exponential behavior. This confirms that the band at

163 nm (7.60 eV) is caused by the host lattice absorption with a subsequent energy transfer to the Ce^{3+} ions.

4. Discussion

Thus, the luminescence properties of Eu^{2+} in Li_2CaGeO_4 and its Si-analog are quite similar, as expected for Eu^{2+} ions occupying positions of very equal dimensions and with the same point symmetry. It is known that the depression in energy position of the lowest $4f^65d$ level of Eu^{2+} ion in a crystal can be considered as a result of two independent contributions, namely the centroid shift E_c, defined as the energy shift of the barycentre of the Eu^{2+} $4f^65d$ configuration relative to the free ion value ($\sim$34,000 cm^{-1}), and the total crystal field splitting E_{cfs}, defined as the energy difference between the maxima of the highest and lowest $4f^7 \rightarrow 4f^65d$ bands in the excitation spectra [16,17]. The value of centroid shift E_c mainly depends on the covalency of the Eu^{2+}–ligand bond and the polarizability of the ligands coordinating Eu^{2+}, whereas the crystal field splitting is determined by the size and shape of the coordination polyhedron around Eu^{2+} [16,17]. The complicated energy level scheme of the Eu^{2+} $4f^65d$ configuration makes the determination of the total crystal splitting and the centroid shift difficult in compounds where, like Li_2CaRO_4, Eu^{2+} ions occupy sites with low point symmetry. By contrast, the 5d configuration of Ce^{3+} ions in a crystal is typically split into five different crystal-filed components, so that five distinct $4f \rightarrow 5d$ bands are usually observed in excitation and absorption spectra of Ce^{3+} ions. Since the centroid shift, the total crystal splitting of the 5d configuration of Eu^{2+} and Ce^{3+} ions in a crystal is generally linearly related to one another [17], luminescence characteristics of Ce^{3+} ions in a compound can be used to explain those of Eu^{2+} in the same compound. The necessary conditions for reasonable conclusions are that in a compound the Ce^{3+} should occupy the same position as Eu^{2+}, and the charge compensating defect should be located outside the first coordination sphere of Ce^{3+}. As mentioned above (see Section 3), these conditions are realized in the case of $Li_2Ca_{1-x}Ce_xGeO_4$ ($x \leq 0.005$).

In Table 1, the luminescence characteristics of Ce^{3+} ions in Li_2CaRO_4 (R = Si, Ge) are compared. It is seen that the total crystal field splitting E_{cfs} for Ce^{3+} ions in Li_2CaGeO_4 (16760 cm^{-1}) is close to, but smaller than typical values for an eightfold coordinated site of D_{2d} symmetry reported in the literature (17,500–18,500 cm^{-1} [16,18]), indicating to a more cubic environment around Ce^{3+}. However, although the positions of the Ce^{3+} lowest excitation band for $Li_2CaSi(Ge)O_4$ are practically the same, this value of E_{cfs} is essentially smaller than that (E_{cfs} = 19,490 cm^{-1}) found for Ce^{3+} ions in Li_2CaSiO_4 by Dorenbos et al. [18]. This unexpected result can be assigned to differences in the coordination polyhedra of the Ce^{3+} ions in these compounds. The magnitude of the tetragonal distortion from perfect cubic structure is also often described by the crystal field splitting parameter Δ, defined as the energy difference between the two lowest sublevels of the 5d configuration [10,19]. The large value of Δ for Ce^{3+} ions in Li_2CaSiO_4 as compared to Li_2CaGeO_4 (8917 cm^{-1} vs. 6559 cm^{-1}) also indicates to a strong distortion of Ce^{3+} surrounding from cubic symmetry in Li_2CaSiO_4. In our opinion, this effect may arise from a local distortion of the lattice caused by the presence of the trivalent lanthanide ions on calcium sites. In general, any change in the cation charge should influence its polyhedron geometry through the corresponding local changes in bond lengths. Unfortunately, quantitative analysis of spectroscopic consequences of this effect requires precise knowledge of the lattice distortions induced by the presence of the impurity ion.

Two groups of authors have performed calculations of the band structure and partial densities of states for Ca_2GeO_4 by means of the density functional theory [11,20]. In spite of the fact that there are distinct differences between the results obtained, one can conclude that the valence-band electronic structure of Ca_2GeO_4 is mainly determined by the O 2p, 2s states, whereas the low conduction band is mostly composed of Ca-states, with some contribution from Ge 4p, 4s states. The calculated band gap energy for Ca_2GeO_4 ($\sim$4.2 eV) was found to be in reasonable agreement with experimental ones of 5.4 eV [11] and 5.58 eV [20]. The features in the 100–150 nm region, observed in the VUV excitation spectra for the Ce^{3+} emission in Ca_2GeO_4, were attributed to the electronic transitions within the GeO_4^{4-} groups [20]. This interpretation coincides with the calculated band gap of germanium dioxide GeO_2 (8.5 eV, 146 nm) [21]. In comparison with Ca_2GeO_4, the threshold of interband transitions in Li_2CaGeO_4 is at the higher energies ($\geq$ 7.0 eV), and, probably, Ge-states are involved in the transitions slightly above the fundamental absorption edge.

5. Conclusions

The luminescence properties of Eu^{2+} ions in Li_2CaGeO_4 have been studied for the first time. The Eu^{2+} ions in Li_2CaGeO_4 exhibit the intense emission with a maximum

Table 1
Comparison of the luminescence properties of Ce^{3+} ions in Li_2CaRO_4 (R = Si, Ge).

Compound	Excitation maxima, nm	E_{cfs}, cm^{-1}	E_c, cm^{-1}	δ, cm^{-1}	Ref.
Li_2CaSiO_4	207, 235, 245, 265, 347	19,490	11,580	2000	[18]
Li_2CaGeO_4	219, 237, 256, 282, 346	16,760	12,640	1580	This work

at 473 nm. The Stokes shift of this emission band is relatively small (820 cm^{-1}), the full-width at half-maximum (1415 cm^{-1}) is typical for $4f^6 5d \rightarrow 4f^7$ transitions of Eu^{2+} in inorganic compounds, so that the luminescence properties of Eu^{2+} in Li_2CaGeO_4 and its Si-analog (Li_2CaSiO_4) are quite similar.

The energies of all 5d crystal field levels of Ce^{3+} ions, values of the crystal field splitting and the centroid shift of the Ce^{3+} 5d configuration in Li_2CaGeO_4 were also determined and compared with those of Ce^{3+} ions in Li_2CaSiO_4. Although the positions of the Ce^{3+} lowest excitation band for Li_2CaRO_4 (R = Si, Ge) are practically the same, the magnitudes of the Ce^{3+} crystal field splitting appeared to be unexpectedly very different. This effect is tentatively attributed to a local distortion of the calcium site in Li_2CaSiO_4 caused by the presence of the trivalent lanthanide ion. In addition to the $4f \rightarrow 5d$ excitation bands, the excitation spectra of the Ce^{3+} and Eu^{2+} ions emissions Li_2CaGeO_4 contain a number of features at wavelengths shorter than 180 nm, which are attributed to the host lattice absorption.

References

[1] H.S. Jang, D.Y. Jeon, White light emission from blue and near ultraviolet light-emitting diodes precoated with a $Sr_3SiO_5:Ce^{3+},Li^+$ phosphors, Optics Letters 32 (2007) 3444–3446.

[2] K. Toda, Y. Kawakami, S. Kousaka, Y. Ito, A. Komeno, K. Uematsu, M. Sato, New silicate phosphors for white LED, IEICE Transactions on Electronics E89-C (2006) 1406–1412.

[3] M. Zhang, J. Wang, W. Ding, Q. Zhang, Q. Su, Luminescence properties of $M_2MgSi_2O_7:Eu^{2+}$ (M = Ca, Sr) phosphors and their effects on yellow and blue LEDs for solid-state lighting, Optical Materials 30 (2007) 571–578.

[4] M. Pardha Saradhi, U.V. Varadaraju, Photoluminescence studies of Eu^{2+}-activated Li_2SrSiO_4—a potential orange–yellow phosphor for solid-state lighting, Chemistry of Materials 18 (2006) 5267–5272.

[5] H. He, R.L. Fu, H. Wang, X. Song, Z. Pan, X. Zhao., X. Zhang, Y. Cao, $Li_2SrSiO_4:Eu^{2+}$ phosphor prepared by the Pechini method and its application in white light emitting diode, Journal of Materials Research 23 (2008) 3288–3294.

[6] M. Xie, H. Liang, Q. Su, Y. Huang, Z. Gao, Y. Tao, Intense cyan-emitting of $Li_2CaSiO_4:Eu^{2+}$ under low-voltage cathode ray excitation, Electrochemical and Solid-State Letters 14 (2011) J69–J72.

[7] V.P. Dotsenko, S.M. Levshov, I.V. Berezovskaya, G.B. Stryganyuk, A.S. Voloshinovskii, N.P. Efryushina, Luminescent properties of Eu^{2+} and Ce^{3+} ions in strontium litho-silicate Li_2SrSiO_4, Journal of Luminescence 131 (2011) 310–315.

[8] X. Zhang, H. He, Z. Li, T. Yu, Z. Zou, Photoluminescence studies on Eu^{2+} and Ce^{3+}-doped Li_2SrSiO_4, Journal of Luminescence 128 (2008) 1876–1879.

[9] S.M. Levshov, I.V. Berezovskaya, N.P. Efryushina, S.I. Vdovenko, I.P. Kovalevskaya, V.P Dotsenko, Luminescence of Eu^{2+} ions in alkaline earth dilithiosilicates, Journal of Applied Spectroscopy 79 (2012) 70–75.

[10] A.A. Setlur, W.J. Heward, Y. Gao, A.M. Srivastava, R.G. Chandran, M.V. Shankar, Crystal chemistry and luminescence of Ce^{3+}-doped $Lu_2CaMg_2(Si, Ge)_3O_{12}$ and its use in LED based lighting, Chemistry of Materials 18 (2006) 3314–3322.

[11] Z. Jiang, Y. Wang, Z. Ci, H. Jiao, Electronic structure and luminescence properties of yellow-emitting $Ca_2GeO_4:Ce^{3+}$, Li^+ phosphor for white light-emitting diodes, Journal of the Electrochemical Society 156 (2009) J317–J320.

[12] M. Jiang-Xin, Y. Chuang-Tao, C. Qing-Qing, Photoluminescence characterization of Ce^{3+} and Dy^{3+} doped Li_2CaGeO_4, Journal of Luminescence 130 (2010) 1320–1323.

[13] J.A. Gard, R. West, Preparation and crystal structure of Li_2CaSiO_4 and isostructural Li_2CaGeO_4, Journal of Solid State Chemistry **7** (1973) 422–427.

[14] E.E. Martsinko, L.Kh. Minacheva, A.G. Pesaroglo, I.I. Seifullina, A.V. Churakov, V.S. Sergienko, Bis(citro)germanates of bivalent 3d metals (Fe,Co,Ni,Cu,Zn). Crystal and molecular structure of $[Fe(H_2O)_6][Ge(HCit)_2] \cdot 4H_2O$, Russian Journal of Inorganic Chemistry 56 (2011) 1243–1249.

[15] G. Zimmerer, SUPERLUMI: a unique setup for luminescence spectroscopy with synchrotron radiation, Radiation Measurements 42 (2007) 859–864.

[16] P. Dorenbos, 5d-level energies of Ce^{3+} and the crystalline environment. III. Oxides containing ionic complexes, Physical Review B 64 (2001) 125117/1–125117/12.

[17] P. Dorenbos, Relation between Eu^{2+} and Ce^{3+} $f \rightarrow d$–transition energies in inorganic compounds, Journal of Physics: Condensed Matter 15 (2003) 4797–4807.

[18] P. Dorenbos, L. Pierron, L. Dinca, C.W.E. van Eijk, A. Kahn-Harari, B. Viana, 4f-5d spectroscopy of Ce^{3+} in $CaBPO_5$, $LiCaPO_4$ and Li_2CaSiO_4, Journal of Physics: Condensed Matter 15 (2003) 511–520.

[19] J.L. Wu, G. Gundiah, A.K. Cheetham, Structure–property correlations in Ce-doped garnet phosphors for use in solid state lighting, Chemical Physics Letters 441 (2007) 250–254.

[20] J. Zhang, M. Zhou, Q. Qin, M. Yu, Y. Wang, The electronic structure and photoluminescence properties of $Ca_2GeO_4:Eu^{3+}$ in ultraviolet and vacuum ultraviolet region, Journal of Luminescence 131 (2011) 1636–1640.

[21] V.B. Sulimov, V.O. Sokolov, B. Poumellec, Cluster modelling of the oxygen vacancy in the SiO_2–GeO_2 system, Physica Status Solidi B 196 (1996) 175–192.